

Fig. S1. Detailed clinical design for the 'ENTICE' canine chronic enteropathy study.

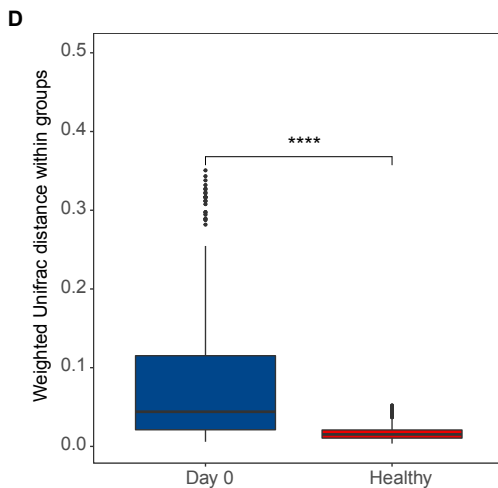
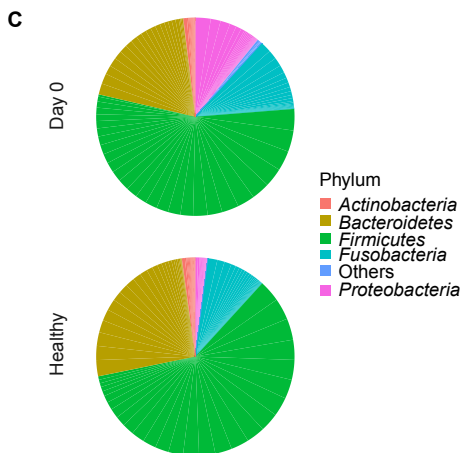
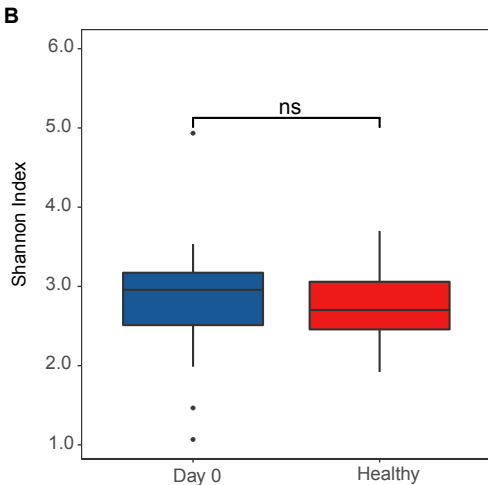
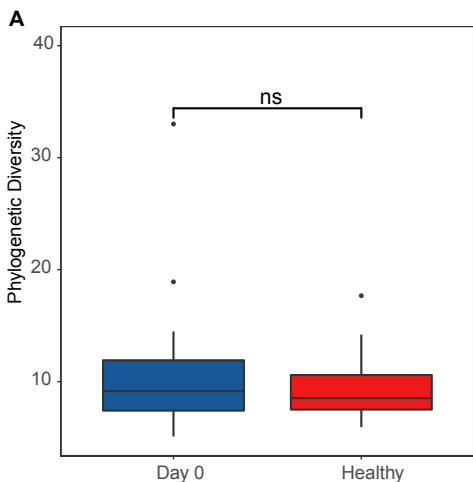


Fig. S2. Community structures of microbiomes in the dogs with CE and in the healthy dogs. Faith's phylogenetic diversity (A) and Shannon index (B) were compared between the samples from the dogs with CE (day 0) and the samples from healthy dogs. (C) The ratios of microbiota compositions at a phylum level. (D) Weighted Unifrac distances within the microbiomes of the dogs with CE or within those of the healthy dogs. ns = not significant, \*\*\*\* $p < 0.0001$  using two-sided Wilcoxon rank sum test.

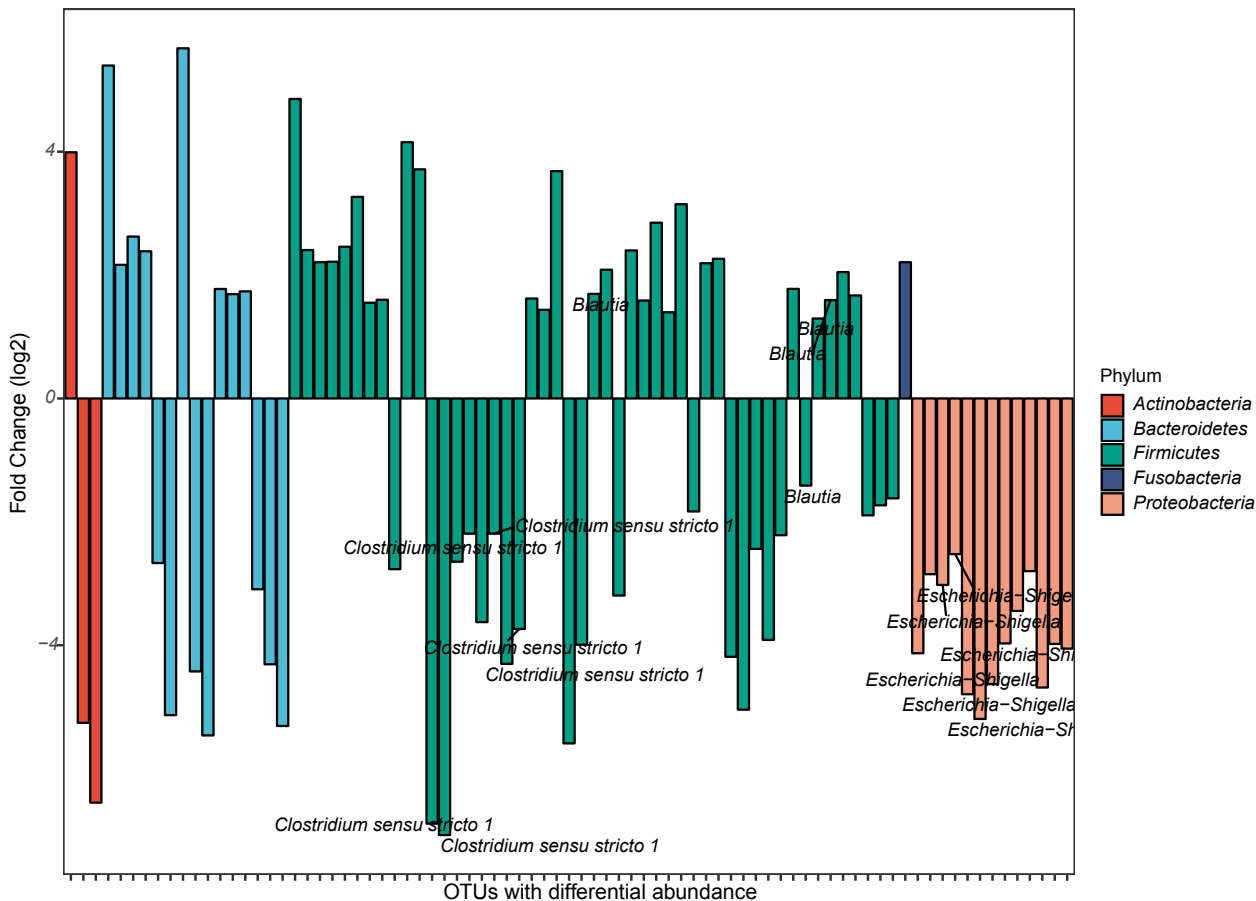


Fig. S3. Differentially abundant OTUs between healthy animals and CE animals. OTUs with differential abundances were identified using DESeq2 ( $\log_2(\text{Fold-Change}) > 1$  and  $P < 0.05$ ). OTUs from *Fusobacteria*, *Firmicutes*, *Actinobacteria*, *Proteobacteria*, and *Bacteroidetes* are shown.

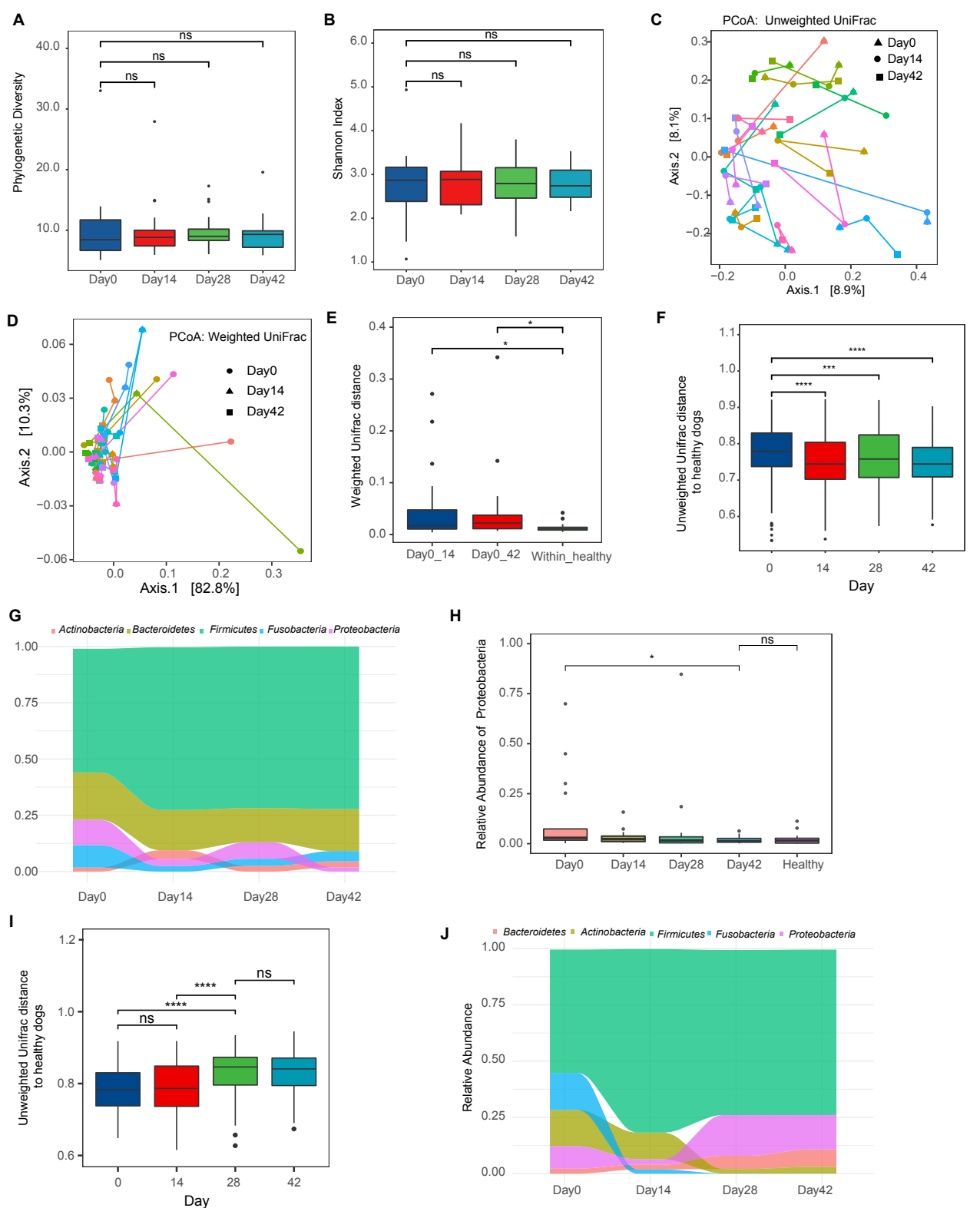


Fig. S4. Microbiota community structure changes induced by diet therapy. (A) Faith's phylogenetic diversity for DR animals. (B) Shannon index for DR animals. (C) Principal coordinate Analysis (PCoA) based on unweighted UniFrac distance or (D) weighted UniFrac distance of the microbiomes from DR animals. (E) Weighted UniFrac distance of microbiomes between samples at different timepoints for each dog in DR group (Day0\_Day14 and Day0\_Day42) and between animals within healthy control (within\_healthy). 'Day0\_Day14' and 'Day0\_Day42' represent the shift of microbiome measured by weighted UniFrac distance from day 0 to day 14, or day 0 to day 42, respectively, for each dog in DR group. 'Within\_healthy' represents the heterogeneity of microbiome within healthy control group. (F) Unweighted UniFrac distance to healthy dogs for DR animals. (G) Stream plot showing phylum level (mean values) dynamics of microbiota structure for DR animals throughout the study. (H) Relative Abundance of the phylum *Proteobacteria* for DR animals after diet and for healthy animals. (I) Unweighted UniFrac distance to healthy dogs for NDR animals. (J) Stream plot showing phylum level (mean values) dynamics of microbiota structure for NDR animals throughout the study. ns = not significant, \* $p < 0.05$ , \*\*\* $p < 0.001$ , \*\*\*\* $p < 0.0001$  using two-sided Wilcoxon rank sum test.

AB031059.1.1463    FP929060.3837.5503    GQ448486.1.1387    HK557089.3.1395    HQ803964.1.1435  
 AM276386.1.1444    GQ138615.1.1402    GQ448506.1.1374    HQ762568.1.1452    JN387556.1.1324  
 DQ113765.1.1450    GQ358246.1.1466    GQ449137.1.1391    HQ762965.1.1448    JN681884.1.1409  
 DQ800757.1.1352    GQ448243.1.1395    GQ491183.1.1360    HQ776819.1.1426    JQ208181.1.1352  
 FJ950694.1.1472    GQ448336.1.1418    GQ491426.1.1332    HQ780723.1.1445    KF842502.1.1392  
 FJ957528.1.1445    GQ448342.1.1392    GQ491616.1.1341    HQ782658.1.1415    KF842617.1.1434  
 FN563300.1.1447    GQ448348.1.1394    GQ493039.1.1311    HQ784885.1.1447    New.ReferenceOTU131  
 FN667422.1.1495    GQ448468.1.1366    GQ493166.1.1359    HQ792937.1.1430    New.ReferenceOTU82

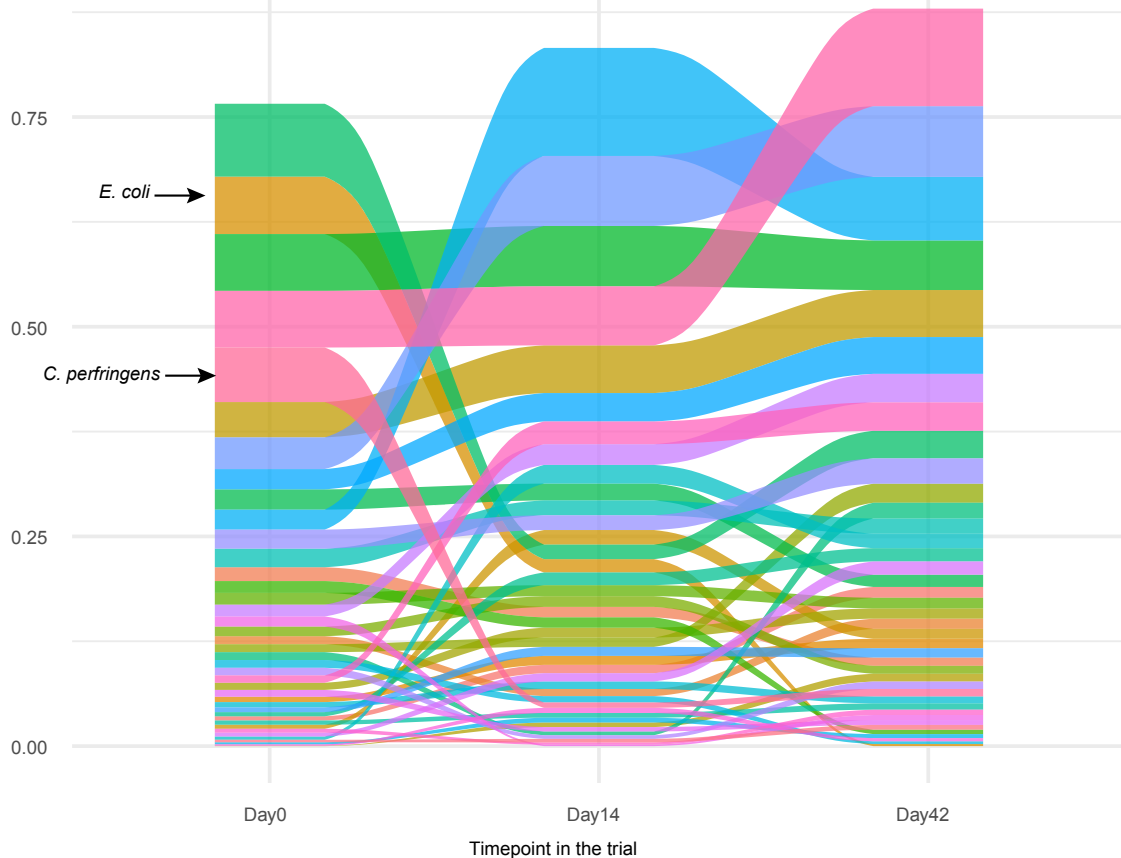


Fig. S5. OTU level (mean values) dynamics of microbiota structure for DR animals throughout the study. Stream plot showing the changes in the relative abundance of the top 40 most abundant OTUs across the timepoints in the ENTICE study. *E. coli* and *C. perfringens* are indicated with arrows.

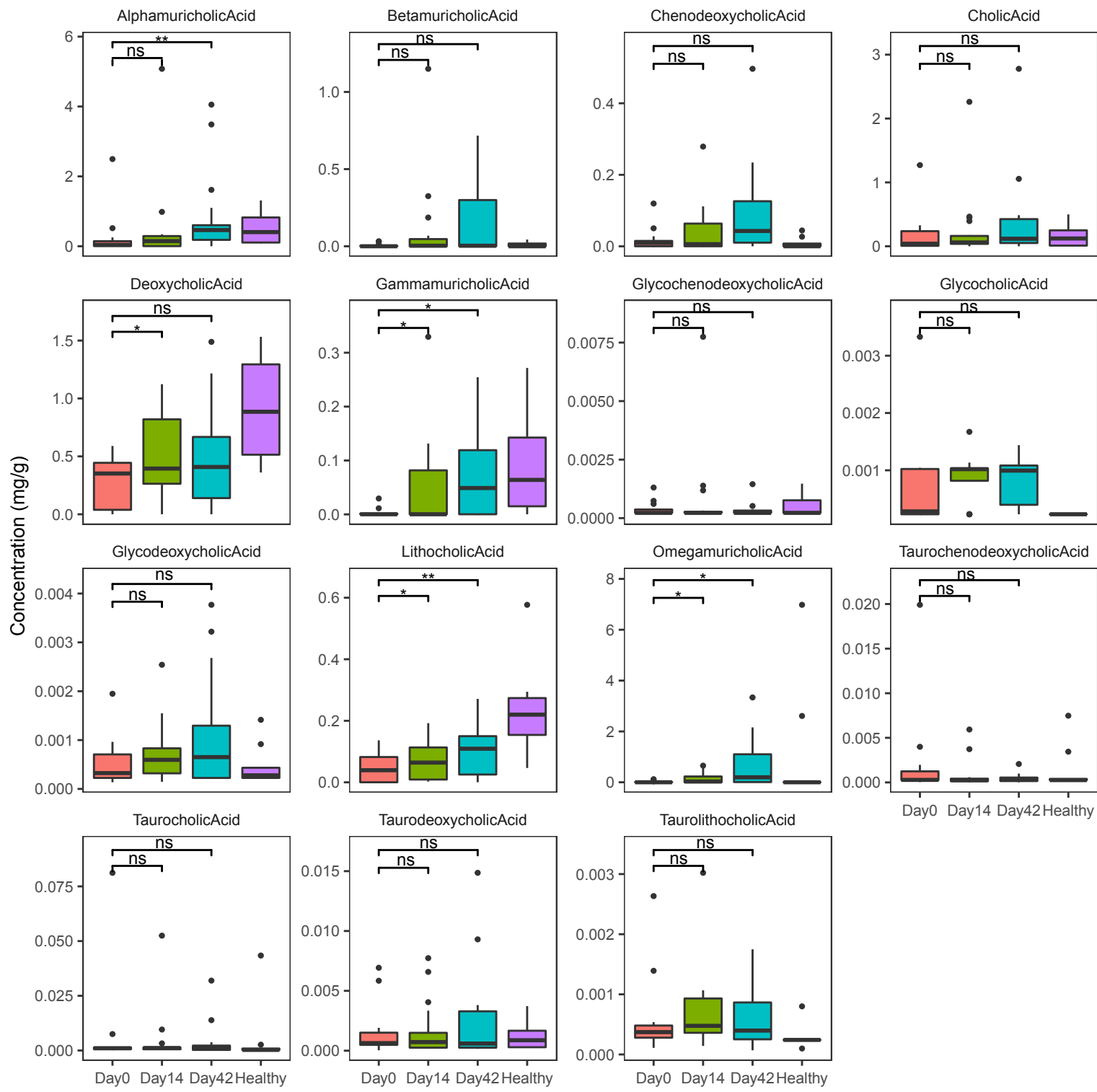


Fig. S6. Concentrations of bile acids detected in fecal samples from diet-responsive dogs. Concentrations (mg/g stool sample) were converted from nmol/g with molecular weights. ns = not significant, \* $p < 0.05$ , \*\* $p < 0.01$  using two-sided Wilcoxon signed-rank test.

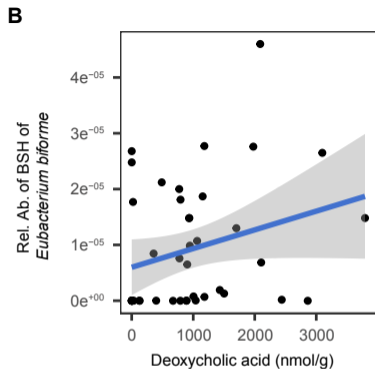
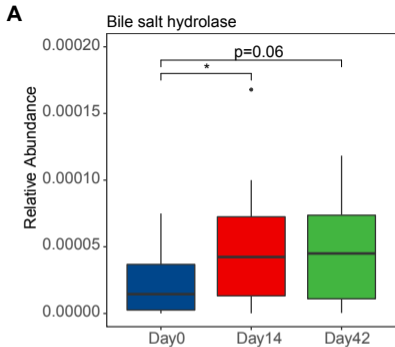


Fig. S7. Bile salt hydrolase (BSH) abundance in DR animals. (A) The relative abundances of BSH gene in DR animals based on metagenomic data. The relative abundance for genes with homology to UniRef 50 reference cluster UniRef50\_Q06115 is shown. (B) Correlation between the relative abundance (Rel. Ab.) of BSH in *Eubacterium bifforme* and deoxycholic acid concentration in stool samples for DR animals. The species-level abundance of BSH was estimated using HUMAnN2. ns = not significant, \* $p < 0.05$ , using two-sided Wilcoxon rank sum test.





*Clostridium hiranonis*

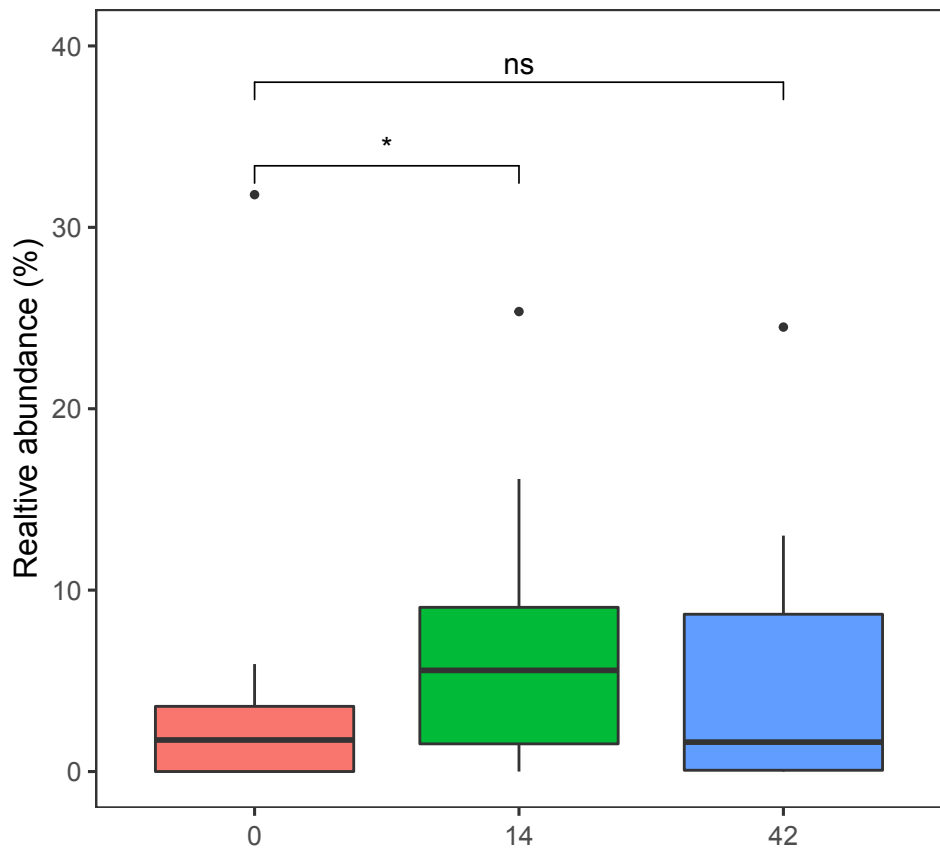
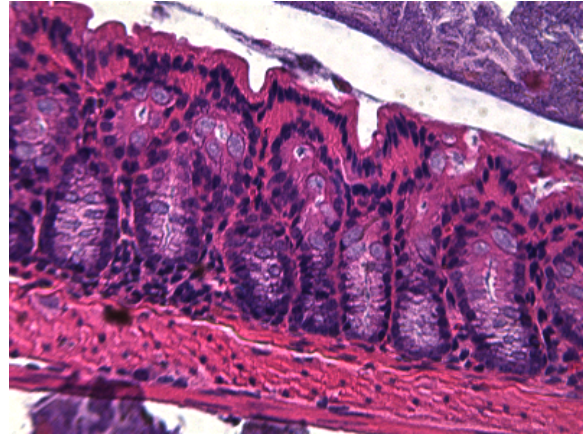
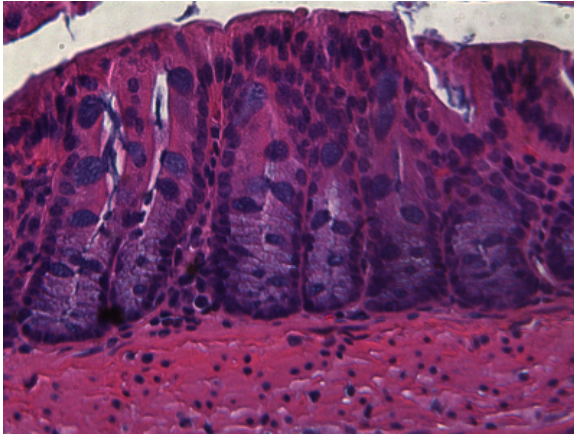


Fig. S9. Relative abundance of *C. hiranonis* in diet responsive dogs calculated from metagenomic data. ns = not significant, \* $p < 0.05$ , using two-sided Wilcoxon signed-rank test.

Vehicle

*C. hiranonis*

Mock



DSS

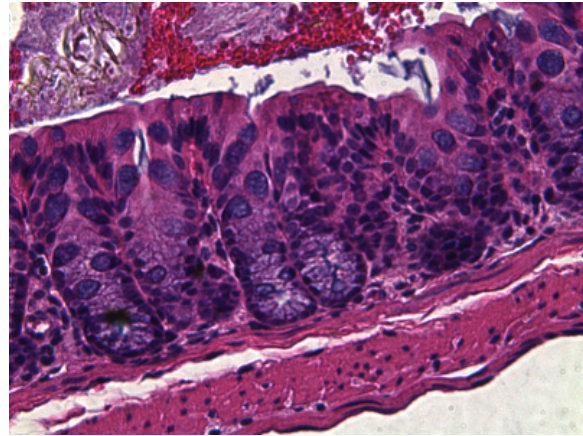
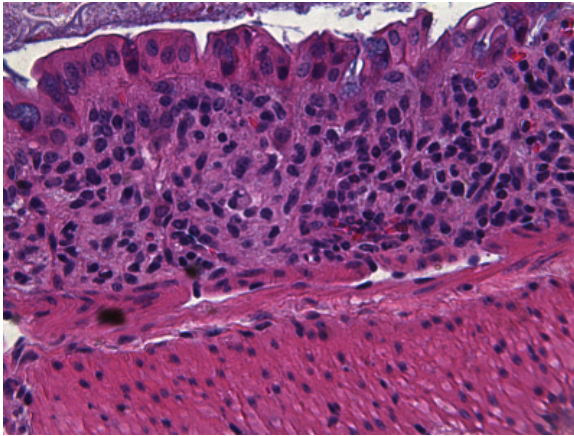


Fig. S10. Representative H&E staining sections of distal colon tissues at day 8 (40 x objective).

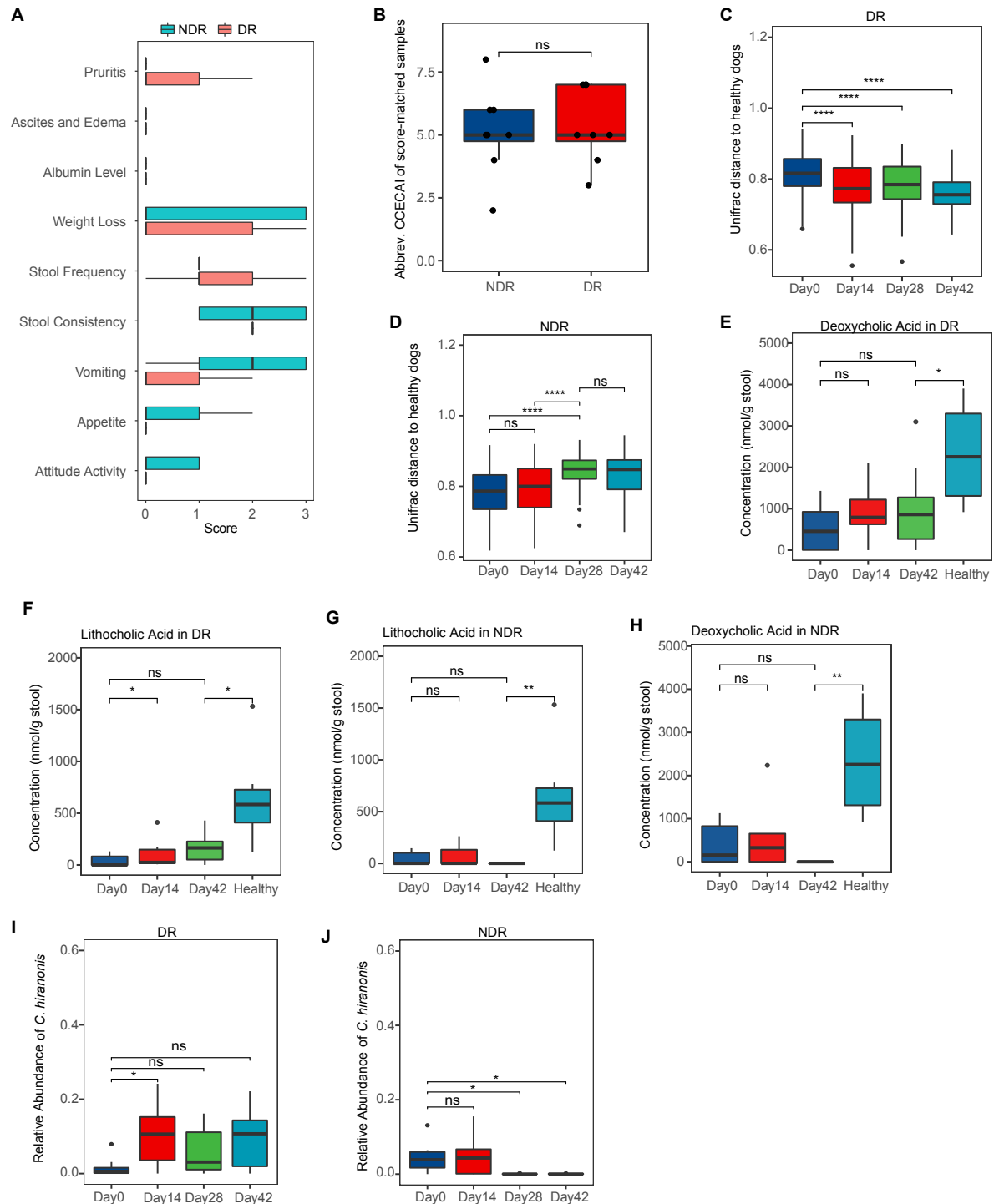


Fig. S11. Disease score-matched analysis. (A) Comparison of CCECAI component scores between DR and NDR animals. (B) CCECAI distribution for animals used in disease scores-matched analysis. (C) Unweighted UniFrac distance of DR group to healthy group. (D) Unweighted UniFrac distance of NDR group to healthy group. Deoxycholic acid levels for (E) DR animals and (H) NDR animals, and lithocholic acid levels for (F) DR animals and (G) NDR animals are shown. (I) Relative abundance of *C. hiranonis* in DR animals and (J) NDR animals. ns = not significant, \* $p < 0.05$ , \*\* $p < 0.01$ , \*\*\*\* $p < 0.0001$  using two-sided Wilcoxon rank sum test for panels B-H or two-sided Wilcoxon signed rank (paired) test for panels I and J.